Peer-reviewed version available at *Int. J. Mol. Sci.* **2019**, *20*, 3284; doi:10.3390/ijms20133284

SerThr-PhosphoProteome of Brain from Aged PINK1-KO+A53T-SNCA Mice Reveals pT1928-MAP1B and pS3781-ANK2 Deficits, as Hub Between Autophagy and Synapse Changes

Georg Auburger[1#], Suzana Gispert[1], Sylvia Torres-Odio[1,2], Marina Jendrach[1,3], Nadine Brehm[1], Júlia Canet-Pons[1], Jana Key[1], Nesli-Ece Sen[1]

[1] Exp. Neurology, Goethe University Medical Faculty, 60590 Frankfurt am Main, Germany

[2] Present address: Department of Microbial Pathogenesis and Immunology, Texas A&M University Health Science Center, College Station, TX, USA

[3] Present address: Department of Neuropathology, Charité - Universitätsmedizin Berlin, corporate member of Freie Universität Berlin, Humboldt-Universität zu Berlin, Berlin Institute of Health, Berlin, Germany.

[#] Corresponding author:

Georg Auburger, Prof. Dr. med., Head of Exp. Neurology,

Neuroscience Center Building 89, Goethe University Medical School,

Theodor Stern Kai 7, 60590 Frankfurt am Main, Germany,

Email: auburger@em.uni-frankfurt.de

Abstract:

Hereditary Parkinson's disease (PD) can be triggered by an autosomal dominant overdose of alpha-Synuclein (SNCA) as stressor or the autosomal recessive deficiency of PINK1 Serine/Threonine-phosphorylation activity as stress-response. We demonstrated the combination of PINK1-knockout with overexpression of $SNCA^{A53T}$ in double mutant (DM) mice to exacerbate locomotor deficits and to reduce lifespan. To survey posttranslational modifications of proteins underlying the pathology, brain hemispheres of old DM mice underwent quantitative label-free global proteomic mass spectrometry, focused on Ser/Thr-phosphorylations. As exceptionally strong effect, we detected >300-fold reductions of phosphoThr1928 in MAP1B, a microtubule-associated protein, and a similar reduction of phosphoSer3781 in ANK2, an interactor of microtubules. MAP1B depletion is known to trigger perturbations of microtubular mitochondria trafficking, neurite extension and synaptic function, so it was noteworthy that relevantly decreased phosphorylation was detected also for other microtubule and microfilament factors, namely $MAP2^{S1801}$, $MARK1^{S394}$, $MAP1A^{T1794}$, $KIF1A^{S1537}$, $4.1N^{S541}$, $4.1G^{S86}$ and $ADD2^{S528}$. While the MAP1B heavy chain supports regeneration and growth cones, its light-chain assists DAPK1-mediated autophagy. Interestingly, relevant phosphorylation decreases of $DAPK2^{S299}$, $VPS13D^{S2429}$ and $VPS13C^{S2480}$ in the DM brain affected regulators of autophagy, which are implicated in PD. Overall, significant downregulations were enriched for PFAM C2 domains, other kinases, and synaptic transmission factors upon automated bioinformatics, while upregulations were not enriched for selective motifs or pathways. Validation experiments confirmed the change of LC3 processing as reflection of excessive autophagy in DM brain, and dependence of ANK2/MAP1B expression on PINK1 levels. Our new data provide independent confirmation in a mouse model with combined PARK1/PARK4/PARK6 pathology that MAP1B/ANK2 phosphorylation events are implicated in Parkinsonian neurodegeneration. These findings expand on previous observations in *D. melanogaster* that the MAP1B ortholog futsch in the presynapse is a primary target of the PARK8 protein LRRK2, and on a report that MAP1B is a component of the pathological Lewy body aggregates in PD patient brains. Similarly, *ANK2* gene locus variants are associated with the risk of PD, ANK2 interacts with PINK1/Parkin-target proteins such as MIRO1 or ATP1A2, and ANK2-derived peptides are potent inhibitors of autophagy.

Keywords: Parkinson's disease; brain phosphorylome; PINK1, alpha-synuclein; microtubular cytoskeleton; autophagy; synaptic signaling

Introduction:

Parkinson's disease (PD) is the second most frequent neurodegenerative disorder. Although its most important risk factor is old age, there are also genetic variants that exacerbate the risk [1]. Indeed, genome-wide surveys have implicated dozens of genes in the pathogenesis, with the biggest impact being due to single nucleotide polymorphisms within the alpha-synuclein gene (gene symbol *SNCA*). Thus, any sporadic PD patient with typical manifestation after the age of 70 years also carries a certain mutation burden. Some 5-10% of patients report a positive family history. Among them, some monogenic traits were identified in rare families across the world. Hereditary variants of PD trigger extremely early manifestation and often rapid progression. The A53T mutation in alpha-synuclein was first identified and is responsible for the PARK1 variant of PD, with onset age around 50 years and autosomal dominant inheritance. Gene triplication and duplication of the alpha-synuclein gene without missense-mutation also causes PD via gene dosage effects, with clinical onset after 30 years and 50 years, respectively. In contrast, a reduced alpha-synuclein dosage protects against PD [2]. Autosomal dominant pedigrees also led to the identification of the LRRK2 gene as the most frequent cause of genetic PD (PARK8), but the manifestation age is usually later and the penetrance is limited, so it is harder to explore the mutation effects in disease models.

Very early onset is observed in juvenile PD with autosomal recessive inheritance. Mutations in the Parkin gene are the most frequent cause identified in cases manifesting around age 25 (the PARK2 variant of PD), mutations in PINK1 are less frequent (the PARK6 variant) [3-5]. Both factors together coordinate mitochondrial quality control after age- or stress-induced damage. Mitochondrial dysfunction leads to the kinase PINK1 becoming abundant at the mitochondrial outer membrane, which starts to phosphorylate ubiquitin and attracts the ubiquitin E3 ligase Parkin from the cytosol [6]. A loss-of-function of PINK1 can be rescued by Parkin [7]. Together, PINK1 and Parkin target the GTPase MIRO to trigger the microtubular removal and autophagic degradation of the damaged mitochondrial segment [8]. Despite their early onset, patients with deficient function of PINK1 and Parkin show slow progression of a typical PD picture and sustained good responses to dopaminergic treatment. Their mild phenotype is exemplified by the good sleep quality of PARK6 patients versus the severe disturbance by REM sleep behavior disorder already at presymptomatic stages in PD cases with dominant synucleinopathy [9, 10]. Also in contrast to PARK2 and PARK6, recessive mutations in other factors like FBXO7 and DNAJC6 that are implicated in protein quality control lead to onset below the age of 11 years and a rapid progression towards an atypical Parkinsonism [11].

Thus, post-translational modifications like the upstream neddylation of PINK1 and Parkin, the phosphorylation activity of PINK1 and the ubiquitylation activity of Parkin are governing the mitochondrial autophagy pathway [12, 13], which is at the heart of typical PD with early-onset autosomal recessive inheritance. Advances in global proteome techniques by mass spectrometry have already made it possible to document the Parkin-dependent ubiquitination events, initially only in tumorous peripheral cell lines [14-17]. Recently we documented the global ubiquitylome of aged brain in Parkin-deleted mice and could thus demonstrate how the altered turnover of neuron-specific factors and disturbed calcium homeostasis combine to impact neural firing frequency [18].

Peer-reviewed version available at *Int. J. Mol. Sci.* **2019**, *20*, 3284; doi:10.3390/ijms20133284

Now, we attempted to define the global phosphorylome in the aged brain from a mouse model of PD, in the hope to identify additional PINK1-controlled proteins. These efforts are important, given that PINK1 is not only controlling mitophagy, but also coordinates the resynthesis of damaged mitochondrial proteins [19], the repair of mitochondria via fusion-fission dynamics [20], mitochondrial apoptosis [21], neuroinflammation [22], and to some degree also bulk autophagy beyond mitochondria [23]. For this phosphorylome survey, we used PINK1-deficient animals that we had generated and characterized, demonstrating that they have mitochondrial dysfunction but no cell loss in their brains within their lifespan [24]. This dysfunction leads to a subtle phenotype involving altered neuronal excitability and calcium homeostasis in corticostriatal projections leading to hypersynchrony, as well as a dysfunction of dopamine release in the midbrain neurons [25-27]. In view of the fact that PINK1 protein is only stable during cell stress periods and that cell culture experiments use mitochondrial uncoupling drugs like CCCP or starvation to maximize PINK1 abundance and subsequent phosphorylation events [28-32], we decided to breed a mitochondrial stress factor into the PINK1-/- mice.

Regarding the role of different stressors, the mitochondrial damage is particularly strong in the flight muscles of *D. melanogaster* flies with ubiquitous PINK1-deletion, due to the continuous energetic stress [33, 34]. A recent mouse study demonstrated that PINK1-/Parkin-dependent neuroinflammation and neurodegeneration can be rescued by deletion of the gene STING, employing PINK1-/Parkin-knockout animals that were stressed either by exhaustive exercise or by crossbreeding with mutator mice with accumulation of mtDNA damage [35]. We favored the crossbreeding with mice that overexpress A53T-alpha-synuclein as stress condition, for several reasons. Firstly, alpha-synuclein is a Parkinson-specific stressor, the main pathogenesis factor in sporadic PD patients where age-associated mitochondrial damage and genetic variants combine to trigger the disease [36]. Secondly, alpha-synuclein has a physiological localization mainly at vesicles, but to some degree also at the interface between mitochondria and endoplasmic reticulum colocalizing with MIRO1, and exerting a powerful mitochondrial stress upon its overexpression [37-40]. Thirdly, patient skin fibroblasts with PINK1-deficiency triggered mitochondrial dysfunction were observed to respond with a transcriptional induction of alpha-synuclein, and PINK1-deficient mice showed enhanced alpha-synuclein immunoreactivity in the brainstem [24, 41-43], so there seems to be a genetic interaction between both factors.

The A53T-SNCA overexpressing mice employed were previously generated and characterized by our team. The animals showed (1) no neuron loss and no alpha-synuclein aggregates upon electron microscopy, but (2) a progressive deficit of spontaneous locomotion and reduced photic entrainment of their spontaneous circadian activity, (3) impaired dopamine signaling and synaptic plasticity in the striatum that could be rescued by the phosphodiesterase inhibitor zaprinast, (4) diminished synaptic vesicle release, (5) elevated intrinsic pacemaker frequency in dopaminergic midbrain neurons, (6) increased postsynaptic sensitivity to apomorpine, (7) expression dysregulation of synaptic vesicle dynamics factors, (8) altered levels of several alpha-synuclein-homologous 14-3-3 isoforms that modulate phosphorylated proteins, and (9) a pathological circadian rhythm [44-53].

Our crossbreeding of PINK1-deficient mice with A53T-SNCA mice reduced survival and potentiated their locomotor deficit, triggering the altered ubiquitination of alpha-synuclein and the increased formation of pSer129-alpha-synuclein aggregates [54]. Beyond the ubiquitylome study in these double-mutant (DM)

Peer-reviewed version available at Int. J. Mol. Sci. 2019, 20, 3284; doi:10.3390/ijms20133284

mice, we performed a systematic characterization of several other post-translational modifications in the global proteome from aged brains, demonstrating (1) that several mitochondrial respiration factors showed an 8-fold reduction of lysine acetylation, and (2) that mitochondrial biogenesis factors showed 1.5-4 fold inductions of arginine methylation [55, 56]. Here, we also assessed the Ser/Thr-phosphorylation events in the global proteome from aged brain in these DM mice.

Materials and Methods:

Breeding and ageing of DM mice, homozygous for Pink1$^{-/-}$ and A53T-SNCA overexpression:
We previously described the generation, ageing and characterization of DM mice [54]. They contain 129/SvEv and FVB/N genetic backgrounds approximately in a 50:50 distribution. As WT control mice we used aged F1-hybrids from a crossbreeding of 129/SvEv and FVB/N mice, which were descended from littermates of the respective single mutant animals. Pairs of DM and WT mice with matched age and male sex were kept in individually ventilated cages under 12 h light cycle with food and water *ad libitum*. Sentinel mice with regular health monitoring including blood tests for viral and parasite infections detected no pathology. The mice under investigation were bred and aged at the FELASA-certified Central Animal Facility (ZFE) of the Frankfurt University Medical School. Housing of animals was in accordance with the German Animal Welfare Act, the Council Directive of 24 November 1986 (86/609/EWG) with Annex II and the ETS123 (European Convention for the Protection of Vertebrate Animals). All the procedures were approved by local animal ethics committee of Regierungspraesidium Darmstadt (ethical code: V54-19c20/15-FK/1083).

Global Phospho-Ser/Thr motif survey by label-free mass-spectrometry:
After decapitation, brain hemispheres from 18-month-old mice (three DM versus three WT animals, matched for male sex) were removed in parallel, snap frozen in liquid nitrogen, stored at −80°C and transported on dry ice to Cell Signaling Technology, Inc. for an outsourced PhosphoScan® procedure [57, 58]. In brief, brain extracts were trypsin-digested and subjected to C18 solid-phase extraction. The lyophilized peptides were immunoprecipitated by protein-A/G-agarose-immobilized mix of Phospho-Ser/Thr antibodies. Peptides were loaded directly onto a 10 cm × 75 µm PicoFrit capillary column packed with Magic C18 AQ reversed-phase resin. The column was developed with a 90-min linear gradient of acetonitrile in 0.125% formic acid delivered at 280 nL/min. The MS parameter settings were as follows: MS Run Time 96 min, MS1 Scan Range (300.0–1500.00), Top 20 MS/MS (Min Signal 500, Isolation Width 2.0, Normalized Coll. Energy 35.0, Activation-Q 0.250, Activation Time 20.0, Lock Mass 371.101237, Charge State Rejection Enabled, Charge State 1+ Rejected, Dynamic Exclusion Enabled, Repeat Count 1, Repeat Duration 35.0, Exclusion List Size 500, Exclusion Duration 40.0, Exclusion Mass Width Relative to Mass, Exclusion Mass Width 10 ppm). MS/MS spectra were evaluated using SEQUEST

3G and the SORCERER 2 platform from Sage-N Research (v4.0, Milpitas, CA, USA) [59]. Searches were performed against the most recent update of the NCBI *Mus musculus* database with mass accuracy of ±50 ppm for precursor ions and 1 Da for product ions. The results were filtered with mass accuracy of ±5 ppm on precursor ions and presence of the intended motif (Phospho-S/T). The peptide identification with relative quantification by mass spectrometry (MS) occurred by LC-MS/MS analysis using LTQ-Orbitrap-VELOS with ESI-CID Sorcerer search.

With double injections of the 6 biological samples, 12 LC-MS/MS experiments were conducted and bioinformatically processed, using the maximum % coefficient of variation (% CV) to control replicate reproducibility. Using a 5% default false-positive rate used to filter the SORCERER results, this procedure yielded a total of 7,508 redundant methylated peptide assignments to 3,526 non-redundant phosphorylated peptides. The quantitative data from the three control WT mice were averaged to compare each DM mouse individually and derive the respective fold-change. The original data are available from the authors upon request.

Bioinformatic pathway enrichment analyses:

For protein-protein-interaction (PPI) network analysis, the software tool STRING (Search tool for the retrieval of interacting genes) v.11.0 (https://string-db.org/) with standard settings was used to visualize networks among factors with >2-fold dysregulation in at least one of the three biological replicates [60]. Automated network statistics were performed; significant functional enrichments of GO (Gene Ontology terms regarding biological processes, molecular functions, cellular components), KEGG pathways, Reactome pathways, PFAM protein domains, INTERPRO Protein Domains and Features, and SMART protein domains were exported into Excel files.

Validation experiments via expression analysis on protein and mRNA level:

Quantitative immunoblots of MAP1B were performed as in the previous description of the DM mice [54], employing the anti-MAP1B antibody from BD Biosciences (catalog # 612678), the anti-ACTB antibody from Sigma (# A5441) and the anti-TUBA antibody from Abcam (# ab15246) at the recommended dilutions. Quantitative RT-PCR was carried out with Taqman assays from Thermofisher (for *PINK1* Hs00260868-m1, for *MAP1B* Hs00195485-m1, for *HPRT1* Hs99999909-m1) again as described [54]. Quantitative immunoblots of LC3 isoforms with the anti-LC3 antibody from Sigma (# L8918) and the culture of primary cortical neurons from 1-4 day old mice with Neurobasal medium over 4 weeks were also done as reported [23].

Results and Discussion:

The global brain proteome of three 18-month-old DM mice versus three age-/sex-matched wildtype (WT) mice was analyzed in a quantitative label-free mass spectrometry approach (see Figure 1) for the abundance of Ser/Thr-phosphorylation motifs (PhosphoScan®). The original data were filtered for consistency and effect size: We excluded factors where each of the three DM mice did not show the same direction of change. We also excluded factors where a two-fold change was not detected at least once among the biological triplicates. The remaining observations comprised 45 factors with relevant phosphorylation downregulations at one or several residues, and 49 factors with relevant upregulations (see Suppl. Table S1).

Strongest downregulations affect microtubular functions:

A massive (>-300-fold) reduction was observed for the uncharacterized phosphorylation-site pT1928 within MAP1B (microtubule-associated protein 1B). This observation reflected a highly specific effect, since many other established phospho-residues in this intensely phosphorylated protein did not exhibit relevant changes: Within MAP1B, eight Ser/Thr-sites are known to be controlled by CDK5, seven by GSK3β, six by p38MAPK, five by CKII, two by CDC2, two by PKA, one each by ERK1 and PKG, while its light chain LC1 and its heavy-chain region containing an 17mer imperfect repeat seem not targeted by these kinases [61]. Known phosphorylations of MAP1B, particularly at the GSK3β-dependent sites pS1260 / pT1265, are mostly located in the interaction domains, where they modulate the stability of microtubules together with the mobility of microfilaments and growth cones [61].

The second biggest reduction (average -3.3-fold) was observed for ANK2 isoforms 2 and 3 (residue pS3781). It appeared even more massive in the analysis of the DM2 mouse (-715-fold) but showed less consistency than MAP1B among the biological triplicates (see Figure 2A). This phospho-site was previously reported to change during long-term potentiation and in fronto-temporal lobar degeneration [62, 63]. Again other established phosphorylation sites in ANK2 that are under control e.g. of CK2 [64] were unchanged. The phosphorylation losses in specific residues of MAP1B and ANK2 seem not to be random effects, since both factors interact physically and exert joint functions. And crucially, the latest systematic investigation of genetic risk factors among >13,000 PD patients and 95,000 control individuals in a genome-wide association study meta-analysis identified the variant rs78738012 next to the *ANK2* gene with high significance (joint p=4.78e−11), providing independent evidence that ANK2 alterations contribute to the pathogenesis of Parkinson's disease.

The association between ANK2 isoforms and MAP1B together with spectrin in *D. melanogaster* was reported to form a membrane-associated microtubule-organizing complex that determines axonal diameter, supports axonal transport, and provides independent control of synaptic dimensions and stability [65-68]. Ankyrins also stabilize the membrane position of Na+/K+ pumps and in particular ANK2 controls ATP1A2 [69, 70], which was recently identified as putative target of Parkin-dependent ubiquitylation [18]. Together, ankyrins with adducin isoforms and the 4.1 protein family link via spectrin onto the actin cytoskeleton, in order to determine the cell surface presence of membrane receptors and channels [71, 72].

Thus it is relevant that ADD2 (beta-adducin) showed a 2.3-fold increase at pS528 and similar upregulations at several subsequent phospho-sites in DM brains (Figure 2A). This putative pathway dysfunction is also supported by the -2.1 fold decrease of pS86 in 4.1G protein (EPB4.1L2) together with 2.2-fold increases of pS541, pS544 and pS546 in 4.1N protein (EPB4.1L1) that were documented in DM brains. The protein 4.1G regulates the membrane presence of the metabolic glutamate receptor mGluR1a, the A1 adenosine receptor, the parathyroid hormone receptor, the sarcoplasmic reticulum Ca^{2+}-ATPase SERCA2, the cell adhesion molecules CADM4 and PTA-1, as well as the high affinity IgG receptor Fc gamma RI (Figure 3A). The protein 4.1N regulates the membrane accumulation of AMPA glutamate receptors GluR1 and GluR4, the dopamine D2 and D3 receptors, the inositol 1,4,5-trisphosphate receptor (ITPR1), the alpha-7 acetylcholine receptor, the K-Cl co-transporter KCC2, as well as the cell adhesion molecules CADM3 and CADM1 [71].

Within the neurite cytosol on the other hand, ANK2 and the established PINK1-/Parkin-target MIRO1 [8] are both required to stabilize APC2 at microtubule branch points and to control the axonal transport of mitochondria to such points within neuronal dendrites [73-76]. Similarly, MAP1B modulates the axonal transport of mitochondria [77], and its light chain LC1 turnover is controlled by the mitophagy regulator MARCH5 [78, 79].

Overall, the phosphorylome survey highlighted a cluster of dysregulations in the cytoskeletal machinery that connects the energy-producing mitochondria with the energy consuming plasma membrane signaling apparatus. The specific strong phosphorylation deficits in MAP1B and ANK2 appear to represent a functional context and were pursued further.

Phospho-residues of MAP1B and ANK2 are conserved and fit with PINK1-target criteria:

The MAP1B site pT1928 is located within the C-terminal part of the heavy chain, which contains twelve repetitions of the 17mer sequence YSYETXEXTTXXPXXXX (aa 1866-2069), whose function is presently not understood. Although there is a lot of sequence variability in this imperfect repeat before the conserved Proline, within the fourth repetition the residue 1928 before the

conserved Proline has a conserved Ser/Thr phosphorylation site according to phylogenetic analyses by CLUSTAL OMEGA (see Figure 2B).

Similarly, the ANK2 residue 3781 also has a conserved Ser phosphorylation site before a conserved Proline (see Figure 2C). Interestingly, it is known that this ANK2 C-terminal regulatory region beyond the DEATH domain is responsible for interaction with specific targets such as ITPR1 or RYR2 to be anchored in the membrane [80].

Importantly, previous *in vitro* analyses have revealed PINK1 to phosphorylate synthetic peptides exclusively at Ser/Thr residues, with strong preference for a neighboring proline at the +1 position [81]. The target sequences TIKT*PED in MAP1B and EESS*PRK in ANK2 both show a proline at the +1 position after each phospho-residue, so they are a good fit with these PINK1 substrate specificity criteria.

Pathway enrichments highlight microtubule functions, synaptic signaling and kinase domains:

MAP1B deficiency alone has several detrimental effects on the microtubule support for synaptic function [82]. It is therefore noteworthy that various other microtubule-related factors showed dysregulated phosphorylation sites in DM brains. The factors MAP2^{S1801}, MARK1^{S394}, MAP1A^{T1794} and KIF1A^{S1537} decreased up to -2.3-fold, while CLASP1^{S646} increased as a factor that tethers microtubules to the extracellular matrix, remodeling microtubules according to signals and damage [83-85] (see Figure 2A). The clustering of phosphorylation dysregulations among factors that constitute the neurite cytoskeleton, their interaction with mitochondria and their anchoring of the membrane signaling machinery was evident, so we attempted to illustrate this subcellular enrichment in Figure 3A. In addition, downregulated phospho-sites were documented for eleven presynaptic (AMPH, BSN, CACNA1B, DNAJC5, CRMP-2, KCNAB1, PICCOLO, RIMS1, STXBP1, SYN3, SYT7) and thirteen postsynaptic (CAMK2B, CAMKV, CPNE6, GABBR2, mGLUR2, HOMER1, OLFR1410, SGIP1, SHANK1, SSTR2, SYT3, TANC2, UNC80) factors (see Suppl. Table S1).

Unbiased automated bioinformatics were employed to identify significant enrichments of protein-protein interactions and established pathways among the dysregulated factors. Indeed, the STRING webtool confirmed that factors with the PFAM C2 domain (as in Protein kinase C isoforms), factors with a Ser/Thr kinase domain, and glutamatergic synapse components were unexpectedly frequent among the downregulations (see Figure 3B and Suppl. Table S2A). Indeed, a total of 11 kinase domain factors showed dysregulation. In contrast, among the upregulation events (see Figure 3C) only the expected enrichments of phosphoproteins and neuronal parts were detected with high significance (Suppl. Table S2B).

Peer-reviewed version available at *Int. J. Mol. Sci.* **2019**, *20*, 3284; doi:10.3390/ijms20133284

Dysregulated phosphorylation of pT1928-MAP1B and of autophagy factors in DM mouse brain:

Beyond automated bioinformatics, it was noted that several autophagy factors showed differential phosphorylation and that these effects may correspond to the role of MAP1B as a positive cofactor in DAPK1-mediated autophagic vesicle formation and membrane blebbing [86, 87]. MAP1B exists in a protein complex that may comprise its heavy-chain, its light-chain LC1, and also MAP1-LC3, which is encoded independently [88]. The LC3 subunit is essential for the formation of autophagosomes and the degradation of mitochondria in distal neuronal axons by the PINK1/Parkin pathway [89, 90], while the MAP1B-LC1 complex can prevent autophagosome formation [91]. The MAP1B-LC1 complex was shown to assist the elimination of cell surface neuronal N-type Ca^{2+} ($Ca_v2.2$) channels [92], and also Parkin influences the degradation of the $Ca_v2.2$ channels [93], so it is interesting to note that pS783-CACNA1B showed a 2-fold increase in DM brain (Suppl. Table S1). Furthermore, the MAP1B light chain LC1 restricts the glutamate receptor AMPA membrane surface presence [94], so again it is noteworthy that pS871 of the glutamate receptor mGluR2 showed a 2-fold increase (Suppl. Table S1). Thus, all three subunits of the MAP1B-LC1-LC3 complex have a differential influence on the turnover of membrane receptors and mitochondria.

Consistent with this impact of MAP1B on DAPK1-dependent autophagy, a relevant phosphorylation deficit (-1.9-fold) occurred for $DAPK2^{S299}$ in DM mouse brain (Suppl. Table S1). Importantly, the VPS13 (Vacuolar Protein Sorting 13) family that regulates autophagy and is implicated in Parkinson's disease or other neurodegenerative processes was also consistently altered. $VPS13D^{S2429}$ showed a strong -3.0-fold downregulation, and $VPS13C^{S2480}$ showed a -2.1-fold decrease. Mutations in VPS13D lead to neurodegeneration in the form of ataxia with spasticity, and VPS13D is required for the regulation of mitochondrial size, fission and autophagic clearance [95-98]. Loss of VPS13C function was reported to cause early-onset autosomal recessive Parkinsonism and to increase PINK1/Parkin-dependent mitophagy [99, 100]. Both show sequence homology to the yeast autophagy regulator ATG2 that mediates lipid transport [101].

Thus, it is unclear if the interaction between cytoskeletal components and the signaling machinery in the plasma membrane is crucial for PD pathogenesis, but clearly PINK1, Parkin and VPS13D all function in the autophagic degradation of mitochondria and all were implicated as risk factors in the pathogenesis of PD. The above data support the notion that VPS13D phosphorylation is downstream from PINK1 kinase activity and A53T-SNCA neurotoxicity.

Known PINK1/SNCA functional effects mirror the roles of dephosphorylated factors in DM brain

The above phosphorylome profile from a PD mouse model cannot be easily validated by independent methods in other brains. PD patient autopsy tissue would show phosphorylation

profiles with distortion due to postmortem delays and due to the loss of specific neuron projections. Frozen brain samples from patients with PINK1 mutation are not available. In the current absence of site-specific antibodies, the detection of the brain phosphorylation events documented above depends on peptide mass spectrometry again in quantitative label-free manner. In aged tissue homogenates, the cell surface accumulation of specific channels / pumps cannot be tested with precision. Furthermore, monitoring the time course or efficiency of mitochondrial autophagy in brain presents formidable challenges. Last but not least, the sizes of MAP1B protein (270 kDa) and ANK2 protein (426 kDa) make their comprehensive assessment in immunoblots and tryptic peptides a cumbersome task.

Even so, it was already demonstrated that neuronal signaling and neurite extension are modified by PINK1 and alpha-synuclein mutations. In a neuronal cell model, the mitochondrial structure and neurite outgrowth were altered by co-expression of alpha-synuclein as stressor together with mutant PINK1 as abnormal stress-response [102]. The overexpression of human alpha-synuclein by itself resulted in reduced neurite extension [103, 104]. This effect was mediated by physical interactions between alpha-synuclein and the cytoskeletal spectrin meshwork [105], and it was dependent on altered activity of glycogen-synthase-kinase-3beta and protein phosphatase 2A [106]. Alpha-synuclein administration to striatal slices leads to a selective redistribution and activation of $Ca_v2.2$ channels [107]. Importantly, it was found that alpha-synuclein associates with MAP1B (previously known as MAP5) and sequestrates it into the pathological aggregates known as Lewy bodies in PD brains [108, 109]. Thus, it is conceivable that the deficient phosphorylation of MAP1B in the DM brain is caused by association of its 17-mer repeat region with pathological alpha-synuclein and consequent masking of the pT1928 site, rather than the loss of PINK1 phosphorylation activity.

Primary mouse neurite retraction is also triggered by mitochondrial damage and PINK1 responses [110]. Dendrite outgrowth in primary neurons could be promoted by the overexpression of wildtype, but not mutant PINK1, even in the absence of its mitochondrial targeting sequence, via enhanced axonal transport of mitochondria and by a Protein-Kinase-A mediated mechanism [111]. In *C. elegans*, the mutation of PINK1 alone was sufficient to alter the mitochondrial structure and axonal outgrowth, phenotypes that could be rescued completely by the deletion of the LRRK2 ortholog [112]. Recently it was shown that the levels of LRRK2 depend on PINK1 [113]. Importantly, LRRK2 in *D. melanogaster* flies was shown to phosphorylate the MAP1B ortholog futsch at the pSer4106 site, far beyond the sequence that is conserved in mammals as C-terminus [114, 115]. It is crucial to note that MAP1B-LC1 was found stably associated with LRRK2 upon yeast-two hybrid studies and that MAP1B-LC1 overexpression rescued LRRK2-mutation triggered cytotoxicity in human neuroblastoma cells [116]. Thus, it is also conceivable as alternative possibilities that the PINK1 deletion is responsible directly for the deficient MAP1B and ANK2 phosphorylation, or indirectly via downstream LRRK2 kinase activity changes. It is noteworthy that LRRK2 contains an Ankyrin-

Peer-reviewed version available at *Int. J. Mol. Sci.* **2019**, *20*, 3284; doi:10.3390/ijms20133284

repeat domain just like ANK2 and like DAPK1. Overall it is unclear at present, which upstream mechanisms are responsible for the deficient phosphorylation of T1928-MAP1B and S3781-ANK2 in DM brains, while the downstream functional effects of SNCA/PINK1 are a good match with the roles of the dephosphorylated protein complexes.

Validation experiments confirm PINK1 to modulate MAP1B/ANK2 and indicate decreased autophagy in DM brain

To validate whether the massive phosphorylation deficits of MAP1B or ANK2 are indeed selective and are not based on a gross loss of protein abundance, quantitative immunoblots were performed in DM brain homogenate. MAP1B and ANK2 levels showed only modest reductions in the RIPA-soluble fraction that mostly contains cytosolic proteins, and no relevant change in the SDS-soluble fraction that contains mostly membrane proteins (Figure 4A/B). These reductions observed upon normalization versus beta-actin (a component of the cortical cytoskeleton) were even stronger upon normalization versus alpha-tubulin (a component of the microtubular cytoskeleton).

To obtain additional evidence whether PINK1 regulates MAP1B and ANK2, we chose to expose a human neural line to starvation stress (rather than to A53T-SNCA overexpression stress) and then examine the PINK1-dependent regulation of *MAP1B* and *ANK2* mRNA during a time-course experiment. A switch from RPMI+FCS medium to HBSS-FCS medium deprives cells of amino acids, serum lipids and growth factors, providing minimal glucose levels, and potently leading to a several-fold increase in PINK1 / Parkin expression [31]. As seen in Figure 4C, this nutrient restriction in SH-SY5Y neuroblastoma cells prompts a phasic two-fold induction of *MAP1B* mRNA with a maximum at 12 h latency, coinciding with the previously reported phasic induction of *PINK1* mRNA. However, this *MAP1B* transcriptional induction cannot be sustained after 8 hours in cells with stable knockdown of *PINK1*, leading to significant deficits at 12 h and 16 h. MAP1B has little expression in adult brain and is needed mostly when neural circuits develop and during regeneration periods [61, 117], so our findings would suggest that MAP1B is less available and pathologically phosphorylated during stress response phases in PD models with PINK1 deficiency. Similarly, the expression of ANK2 mRNA was induced two/three-fold by starvation stress with significance at 8 h and remained elevated until 48 h. In cells with stable knockdown of *PINK1*, the starvation protocol failed to induce *ANK2* mRNA induction, leading to significant genotype-dependent differences from 8 h to 48 h. This massive dependence of *ANK2* induction on *PINK1* levels during starvation stress is very interesting in the light of two previous reports. Firstly, the deficiency of an Ankyrin-repeat containing *Drosophila* protein was shown to rescue mitochondrial pathology and phenotypes triggered by PINK1 and Parkin mutations [118]. Secondly, peptides derived from ANK2 were observed to be potent and specific inhibitors of autophagy via ATG8-binding [119, 120].

Peer-reviewed version available at *Int. J. Mol. Sci.* **2019**, *20*, 3284; doi:10.3390/ijms20133284

It seems clear that neurite extension and neural signaling are altered in DM brains, but it remained questionable to what degree autophagy is abnormal. While several autophagy modulators, particularly VPS13C as PD risk factor, showed altered phosphorylation in DM brain, it cannot be distinguished whether this phosphorylome profile reflects pathology in the autophagic pathway or a successful homeostatic compensation. On the one hand, the A53T-SNCA overexpression would be predicted to enhance the autophagic degradation of protein aggregates, while on the other hand the formation of autophagosomes and the initiation of degradation might be impaired by PINK1 deletion via Beclin as well as by MAP1B/ANK2 dysfunction via LC3/ATG8. Thus, we used DM brain tissue to assess the conversion of LC3 from the microtubule-associated isoform I to the autophagosome-associated isoform II. Although the LC3-II/I ratio cannot predict how efficiently autophagosome will fuse with lysosomes and degrade the toxic material (therefore cell culture experiments with drugs like Bafilomycin A1 are recommended to test autophagic flux), in tissue and untreated cells this ratio is a reliable marker of autophagosome abundance [121]. Again, HBSS medium was used to deprive DM primary cortical neurons from nutrients and thus trigger autophagy. After 2 h of starvation, quantitative immunoblots of DM cells showed a significantly smaller LC3II/I ratio (reduction to 48%, p=0.0016) (Figure 4C). These findings suggest that the PINK1 deletion impairs autophagosome formation and the clearance of damaged mitochondria as well as toxic protein aggregates. Our observations are in agreement with previous reports from a neuroblastoma cell line where PINK1 deficiency was impairing bulk autophagy [23]. The data also agree with previous findings that phosphorylated MAP1B is associated with autophagosomes [122] and that a reduction of MAP1B will attenuate DAPK1-mediated autophagy [86]. While LC3 is a requirement for autophagosome-mediated degradation, the LC1 fragment of MAP1B prevents autophagosome formation according to recent insights [91]. Therefore it would be interesting in the future to generate neural cells with MAP1B-KnockIn of the phospho-dead T1928A residue versus the phospho-mimetic T1928E residue, to analyze whether absence of this specific phosphorylation event modulates the LC1 cleavage or the autophagosome association of MAP1B.

Conclusion:

DM mouse brains with A53T-SNCA overexpression as stressor and with PINK1 deletion to impair stress-responses were employed in a pioneer Ser/Thr-phosphorylome survey by quantitative label-free mass spectrometry. This approach documented a prominent massive deficit of pT1928-MAP1B, a strong deficit of pS3781-ANK2, and a cluster of dephosphorylation events at cytoskeletal anchors of the synaptic signaling machinery, of mitochondria, or of autophagosomes. The MAP1B and ANK2 dephosphorylation sites show strong phylogenetic

conservation and adhere to the sequence preference of PINK1 kinase. Validation experiments provided additional evidence that MAP1B is modulated by PINK1 and that reduced autophagosome availability exists in DM neurons. Our findings for the first time identify neuron-specific factors that are regulated in similar manner as other known ubiquitous mitophagy and cytoskeleton components, thus shedding light on the selective vulnerability of aged neuron populations. Preferential expression in neurons is particularly known for ANK2, 4.1N and ADD2, but is somewhat true also for MAP2, MARK1, MAP1A and KIF1A. In contrast, mitochondrial components like VDAC3, or cytosolic factors like MIRO1, MAP1B, VPS13C and CLASP1 are similarly expressed in many different tissues. The dephosphorylated factors in DM brain have roles, which are in good agreement with previously observed functional deficits of PD models with PINK1 deficiency or/and SNCA neurotoxicity. Overall, the documented Ser-/Thr-phospho-profile may be useful as biomarker to assess the benefit of novel neuroprotective drugs, but also to identify crucial molecular targets of preventive treatment. It is important to note that MAP1B is already known as physical interactor protein of alpha-synuclein, is also known as target of LRRK2 phosphorylation, and now appears a candidate for PINK1-dependent phosphorylation. Furthermore, ANK2 genetic variants contribute to the risk to develop PD and given that ANK2 also appears as potential target of PINK1-dependent phosphorylation, we now propose to conduct further investigations into the role of MAP1B with its T1828 residue and ANK2 with its S528 residue in the pathogenesis of PD.

Literature:

1. Corti, O. et al. (2011) What genetics tells us about the causes and mechanisms of Parkinson's disease. Physiological reviews 91 (4), 1161-218.
2. Cabin, D.E. et al. (2005) Exacerbated synucleinopathy in mice expressing A53T SNCA on a Snca null background. Neurobiology of aging 26 (1), 25-35.
3. Valente, E.M. et al. (2004) Hereditary early-onset Parkinson's disease caused by mutations in PINK1. Science 304 (5674), 1158-60.
4. Bonifati, V. (2012) Autosomal recessive parkinsonism. Parkinsonism & related disorders 18 Suppl 1, S4-6.
5. Kitada, T. et al. (1998) Mutations in the parkin gene cause autosomal recessive juvenile parkinsonism. Nature 392 (6676), 605-8.
6. Koyano, F. et al. (2014) Ubiquitin is phosphorylated by PINK1 to activate parkin. Nature 510 (7503), 162-6.
7. Exner, N. et al. (2007) Loss-of-function of human PINK1 results in mitochondrial pathology and can be rescued by parkin. The Journal of neuroscience : the official journal of the Society for Neuroscience 27 (45), 12413-8.
8. Wang, X. et al. (2011) PINK1 and Parkin target Miro for phosphorylation and degradation to arrest mitochondrial motility. Cell 147 (4), 893-906.
9. Tuin, I. et al. (2008) Sleep quality in a family with hereditary parkinsonism (PARK6). Sleep medicine 9 (6), 684-8.

10. Lahut, S. et al. (2017) Blood RNA biomarkers in prodromal PARK4 and rapid eye movement sleep behavior disorder show role of complexin 1 loss for risk of Parkinson's disease. Disease models & mechanisms 10 (5), 619-631.
11. Scott, L. et al. (2017) Trumping neurodegeneration: Targeting common pathways regulated by autosomal recessive Parkinson's disease genes. Experimental neurology 298 (Pt B), 191-201.
12. Durcan, T.M. and Fon, E.A. (2015) The three 'P's of mitophagy: PARKIN, PINK1, and post-translational modifications. Genes & development 29 (10), 989-99.
13. Choo, Y.S. et al. (2012) Regulation of parkin and PINK1 by neddylation. Human molecular genetics 21 (11), 2514-23.
14. Ordureau, A. et al. (2015) Defining roles of PARKIN and ubiquitin phosphorylation by PINK1 in mitochondrial quality control using a ubiquitin replacement strategy. Proceedings of the National Academy of Sciences of the United States of America 112 (21), 6637-42.
15. Ordureau, A. et al. (2015) Quantifying ubiquitin signaling. Molecular cell 58 (4), 660-76.
16. Ordureau, A. et al. (2018) Dynamics of PARKIN-Dependent Mitochondrial Ubiquitylation in Induced Neurons and Model Systems Revealed by Digital Snapshot Proteomics. Molecular cell 70 (2), 211-227 e8.
17. Sarraf, S.A. et al. (2013) Landscape of the PARKIN-dependent ubiquitylome in response to mitochondrial depolarization. Nature 496 (7445), 372-6.
18. Key, J. et al. (2019) Ubiquitylome profiling of Parkin-null brain reveals dysregulation of calcium homeostasis factors ATP1A2, Hippocalcin and GNA11, reflected by altered firing of noradrenergic neurons. Neurobiology of disease.
19. Gehrke, S. et al. (2015) PINK1 and Parkin control localized translation of respiratory chain component mRNAs on mitochondria outer membrane. Cell metabolism 21 (1), 95-108.
20. Mai, S. et al. (2010) Decreased expression of Drp1 and Fis1 mediates mitochondrial elongation in senescent cells and enhances resistance to oxidative stress through PINK1. Journal of cell science 123 (Pt 6), 917-26.
21. Klinkenberg, M. et al. (2010) Enhanced vulnerability of PARK6 patient skin fibroblasts to apoptosis induced by proteasomal stress. Neuroscience 166 (2), 422-34.
22. Torres-Odio, S. et al. (2017) Progression of pathology in PINK1-deficient mouse brain from splicing via ubiquitination, ER stress, and mitophagy changes to neuroinflammation. Journal of neuroinflammation 14 (1), 154.
23. Parganlija, D. et al. (2014) Loss of PINK1 impairs stress-induced autophagy and cell survival. PloS one 9 (4), e95288.
24. Gispert, S. et al. (2009) Parkinson phenotype in aged PINK1-deficient mice is accompanied by progressive mitochondrial dysfunction in absence of neurodegeneration. PloS one 4 (6), e5777.
25. Dehorter, N. et al. (2012) Subthalamic lesion or levodopa treatment rescues giant GABAergic currents of PINK1-deficient striatum. The Journal of neuroscience : the official journal of the Society for Neuroscience 32 (50), 18047-53.
26. Carron, R. et al. (2014) Early hypersynchrony in juvenile PINK1(-)/(-) motor cortex is rescued by antidromic stimulation. Frontiers in systems neuroscience 8, 95.
27. Pearlstein, E. et al. (2016) Abnormal Development of Glutamatergic Synapses Afferent to Dopaminergic Neurons of the Pink1(-/-) Mouse Model of Parkinson's Disease. Frontiers in cellular neuroscience 10, 168.
28. Zhou, C. et al. (2008) The kinase domain of mitochondrial PINK1 faces the cytoplasm. Proceedings of the National Academy of Sciences of the United States of America 105 (33), 12022-7.
29. Vives-Bauza, C. et al. (2010) PINK1-dependent recruitment of Parkin to mitochondria in mitophagy. Proceedings of the National Academy of Sciences of the United States of America 107 (1), 378-83.
30. Narendra, D. et al. (2008) Parkin is recruited selectively to impaired mitochondria and promotes their autophagy. The Journal of cell biology 183 (5), 795-803.

31. Klinkenberg, M. et al. (2012) Restriction of trophic factors and nutrients induces PARKIN expression. Neurogenetics 13 (1), 9-21.
32. Jendrach, M. et al. (2009) The mitochondrial kinase PINK1, stress response and Parkinson's disease. Journal of bioenergetics and biomembranes 41 (6), 481-6.
33. Park, J. et al. (2006) Mitochondrial dysfunction in Drosophila PINK1 mutants is complemented by parkin. Nature 441 (7097), 1157-61.
34. Clark, I.E. et al. (2006) Drosophila pink1 is required for mitochondrial function and interacts genetically with parkin. Nature 441 (7097), 1162-6.
35. Sliter, D.A. et al. (2018) Parkin and PINK1 mitigate STING-induced inflammation. Nature 561 (7722), 258-262.
36. Chang, D. et al. (2017) A meta-analysis of genome-wide association studies identifies 17 new Parkinson's disease risk loci. Nature genetics 49 (10), 1511-1516.
37. Guardia-Laguarta, C. et al. (2014) alpha-Synuclein is localized to mitochondria-associated ER membranes. The Journal of neuroscience : the official journal of the Society for Neuroscience 34 (1), 249-59.
38. Kamp, F. et al. (2010) Inhibition of mitochondrial fusion by alpha-synuclein is rescued by PINK1, Parkin and DJ-1. The EMBO journal 29 (20), 3571-89.
39. Menges, S. et al. (2017) Alpha-synuclein prevents the formation of spherical mitochondria and apoptosis under oxidative stress. Scientific reports 7, 42942.
40. Melo, T.Q. et al. (2018) Alpha-Synuclein Toxicity on Protein Quality Control, Mitochondria and Endoplasmic Reticulum. Neurochemical research 43 (12), 2212-2223.
41. Hoepken, H.H. et al. (2008) Parkinson patient fibroblasts show increased alpha-synuclein expression. Experimental neurology 212 (2), 307-13.
42. Hoepken, H.H. et al. (2007) Mitochondrial dysfunction, peroxidation damage and changes in glutathione metabolism in PARK6. Neurobiology of disease 25 (2), 401-11.
43. Auburger, G. et al. (2012) Primary skin fibroblasts as a model of Parkinson's disease. Molecular neurobiology 46 (1), 20-7.
44. Gispert, S. et al. (2003) Transgenic mice expressing mutant A53T human alpha-synuclein show neuronal dysfunction in the absence of aggregate formation. Molecular and cellular neurosciences 24 (2), 419-29.
45. Kurz, A. et al. (2010) A53T-alpha-synuclein overexpression impairs dopamine signaling and striatal synaptic plasticity in old mice. PloS one 5 (7), e11464.
46. Tozzi, A. et al. (2012) Mechanisms underlying altered striatal synaptic plasticity in old A53T-alpha synuclein overexpressing mice. Neurobiology of aging 33 (8), 1792-9.
47. Platt, N.J. et al. (2012) Striatal dopamine transmission is subtly modified in human A53Talpha-synuclein overexpressing mice. PloS one 7 (5), e36397.
48. Subramaniam, M. et al. (2014) Mutant alpha-synuclein enhances firing frequencies in dopamine substantia nigra neurons by oxidative impairment of A-type potassium channels. The Journal of neuroscience : the official journal of the Society for Neuroscience 34 (41), 13586-99.
49. Brehm, N. et al. (2015) A Genetic Mouse Model of Parkinson's Disease Shows Involuntary Movements and Increased Postsynaptic Sensitivity to Apomorphine. Molecular neurobiology 52 (3), 1152-1164.
50. Kurz, A. et al. (2012) A53T-alpha-synuclein-overexpression in the mouse nigrostriatal pathway leads to early increase of 14-3-3 epsilon and late increase of GFAP. Journal of neural transmission 119 (3), 297-312.
51. Brehm, N. et al. (2015) Age-Related Changes of 14-3-3 Isoforms in Midbrain of A53T-SNCA Overexpressing Mice. Journal of Parkinson's disease 5 (3), 595-604.
52. Gispert, S. et al. (2015) Complexin-1 and Foxp1 Expression Changes Are Novel Brain Effects of Alpha-Synuclein Pathology. Molecular neurobiology 52 (1), 57-63.

53. Pfeffer, M. et al. (2018) Impaired Photic Entrainment of Spontaneous Locomotor Activity in Mice Overexpressing Human Mutant alpha-Synuclein. International journal of molecular sciences 19 (6).
54. Gispert, S. et al. (2015) Potentiation of neurotoxicity in double-mutant mice with Pink1 ablation and A53T-SNCA overexpression. Human molecular genetics 24 (4), 1061-76.
55. Auburger, G. et al. (2014) Mitochondrial acetylation and genetic models of Parkinson's disease. Progress in molecular biology and translational science 127, 155-82.
56. Auburger, G. et al. (2016) Methyl-Arginine Profile of Brain from Aged PINK1-KO+A53T-SNCA Mice Suggests Altered Mitochondrial Biogenesis. Parkinson's disease 2016, 4686185.
57. Rush, J. et al. (2005) Immunoaffinity profiling of tyrosine phosphorylation in cancer cells. Nature biotechnology 23 (1), 94-101.
58. Guo, A. et al. (2014) Immunoaffinity enrichment and mass spectrometry analysis of protein methylation. Molecular & cellular proteomics : MCP 13 (1), 372-87.
59. Lundgren, D.H. et al. (2009) Protein identification using Sorcerer 2 and SEQUEST. Current protocols in bioinformatics / editoral board, Andreas D. Baxevanis ... [et al.] Chapter 13, Unit 13 3.
60. Franceschini, A. et al. (2013) STRING v9.1: protein-protein interaction networks, with increased coverage and integration. Nucleic acids research 41 (Database issue), D808-15.
61. Riederer, B.M. (2007) Microtubule-associated protein 1B, a growth-associated and phosphorylated scaffold protein. Brain research bulletin 71 (6), 541-58.
62. Li, J. et al. (2016) Long-term potentiation modulates synaptic phosphorylation networks and reshapes the structure of the postsynaptic interactome. Science signaling 9 (440), rs8.
63. Herskowitz, J.H. et al. (2010) Phosphoproteomic analysis reveals site-specific changes in GFAP and NDRG2 phosphorylation in frontotemporal lobar degeneration. Journal of proteome research 9 (12), 6368-79.
64. Bulat, V. et al. (2014) Presynaptic CK2 promotes synapse organization and stability by targeting Ankyrin2. The Journal of cell biology 204 (1), 77-94.
65. Stephan, R. et al. (2015) Hierarchical microtubule organization controls axon caliber and transport and determines synaptic structure and stability. Developmental cell 33 (1), 5-21.
66. Migh, E. et al. (2018) Microtubule organization in presynaptic boutons relies on the formin DAAM. Development 145 (6).
67. Koch, I. et al. (2008) Drosophila ankyrin 2 is required for synaptic stability. Neuron 58 (2), 210-22.
68. Bennett, V. and Walder, K. (2015) Evolution in action: giant ankyrins awake. Developmental cell 33 (1), 1-2.
69. Nelson, W.J. and Hammerton, R.W. (1989) A membrane-cytoskeletal complex containing Na+,K+-ATPase, ankyrin, and fodrin in Madin-Darby canine kidney (MDCK) cells: implications for the biogenesis of epithelial cell polarity. The Journal of cell biology 108 (3), 893-902.
70. Mohler, P.J. et al. (2003) Ankyrin-B mutation causes type 4 long-QT cardiac arrhythmia and sudden cardiac death. Nature 421 (6923), 634-9.
71. Baines, A.J. et al. (2014) The Protein 4.1 family: hub proteins in animals for organizing membrane proteins. Biochimica et biophysica acta 1838 (2), 605-19.
72. Baines, A.J. (2010) The spectrin-ankyrin-4.1-adducin membrane skeleton: adapting eukaryotic cells to the demands of animal life. Protoplasma 244 (1-4), 99-131.
73. Weiner, A.T. et al. (2018) Identification of Proteins Required for Precise Positioning of Apc2 in Dendrites. G3 8 (5), 1841-1853.
74. Liu, S. et al. (2012) Parkinson's disease-associated kinase PINK1 regulates Miro protein level and axonal transport of mitochondria. PLoS genetics 8 (3), e1002537.
75. Shlevkov, E. et al. (2016) Miro phosphorylation sites regulate Parkin recruitment and mitochondrial motility. Proceedings of the National Academy of Sciences of the United States of America 113 (41), E6097-E6106.

76. Lopez-Domenech, G. et al. (2018) Miro proteins coordinate microtubule- and actin-dependent mitochondrial transport and distribution. The EMBO journal 37 (3), 321-336.
77. Jimenez-Mateos, E.M. et al. (2006) Role of MAP1B in axonal retrograde transport of mitochondria. The Biochemical journal 397 (1), 53-9.
78. Nagashima, S. et al. (2014) Roles of mitochondrial ubiquitin ligase MITOL/MARCH5 in mitochondrial dynamics and diseases. Journal of biochemistry 155 (5), 273-9.
79. Chen, Z. et al. (2017) MARCH5-FUNDC1 axis fine-tunes hypoxia-induced mitophagy. Autophagy 13 (7), 1244-1245.
80. Mohler, P.J. et al. (2002) The ankyrin-B C-terminal domain determines activity of ankyrin-B/G chimeras in rescue of abnormal inositol 1,4,5-trisphosphate and ryanodine receptor distribution in ankyrin-B (-/-) neonatal cardiomyocytes. The Journal of biological chemistry 277 (12), 10599-607.
81. Woodroof, H.I. et al. (2011) Discovery of catalytically active orthologues of the Parkinson's disease kinase PINK1: analysis of substrate specificity and impact of mutations. Open biology 1 (3), 110012.
82. Bodaleo, F.J. et al. (2016) Microtubule-associated protein 1B (MAP1B)-deficient neurons show structural presynaptic deficiencies in vitro and altered presynaptic physiology. Scientific reports 6, 30069.
83. Stehbens, S.J. et al. (2014) CLASPs link focal-adhesion-associated microtubule capture to localized exocytosis and adhesion site turnover. Nature cell biology 16 (6), 561-73.
84. Galjart, N. (2005) CLIPs and CLASPs and cellular dynamics. Nature reviews. Molecular cell biology 6 (6), 487-98.
85. Al-Bassam, J. and Chang, F. (2011) Regulation of microtubule dynamics by TOG-domain proteins XMAP215/Dis1 and CLASP. Trends in cell biology 21 (10), 604-14.
86. Harrison, B. et al. (2008) DAPK-1 binding to a linear peptide motif in MAP1B stimulates autophagy and membrane blebbing. The Journal of biological chemistry 283 (15), 9999-10014.
87. Capoccia, B.J. et al. (2013) The ubiquitin ligase Mindbomb 1 coordinates gastrointestinal secretory cell maturation. The Journal of clinical investigation 123 (4), 1475-91.
88. Mann, S.S. and Hammarback, J.A. (1994) Molecular characterization of light chain 3. A microtubule binding subunit of MAP1A and MAP1B. The Journal of biological chemistry 269 (15), 11492-7.
89. Ashrafi, G. et al. (2014) Mitophagy of damaged mitochondria occurs locally in distal neuronal axons and requires PINK1 and Parkin. The Journal of cell biology 206 (5), 655-70.
90. Lee, Y.K. and Lee, J.A. (2016) Role of the mammalian ATG8/LC3 family in autophagy: differential and compensatory roles in the spatiotemporal regulation of autophagy. BMB reports 49 (8), 424-30.
91. Arasaki, K. et al. (2018) MAP1B-LC1 prevents autophagosome formation by linking syntaxin 17 to microtubules. EMBO reports 19 (8).
92. Gandini, M.A. et al. (2014) The MAP1B-LC1/UBE2L3 complex catalyzes degradation of cell surface CaV2.2 channels. Channels 8 (5), 452-7.
93. Grimaldo, L. et al. (2017) Involvement of Parkin in the ubiquitin proteasome system-mediated degradation of N-type voltage-gated Ca2+ channels. PloS one 12 (9), e0185289.
94. Palenzuela, R. et al. (2017) MAP1B Light Chain Modulates Synaptic Transmission via AMPA Receptor Intracellular Trapping. The Journal of neuroscience : the official journal of the Society for Neuroscience 37 (41), 9945-9963.
95. Cao, X. et al. (2017) In vivo imaging reveals mitophagy independence in the maintenance of axonal mitochondria during normal aging. Aging cell 16 (5), 1180-1190.
96. Anding, A.L. et al. (2018) Vps13D Encodes a Ubiquitin-Binding Protein that Is Required for the Regulation of Mitochondrial Size and Clearance. Current biology : CB 28 (2), 287-295 e6.
97. Seong, E. et al. (2018) Mutations in VPS13D lead to a new recessive ataxia with spasticity and mitochondrial defects. Annals of neurology 83 (6), 1075-1088.
98. Gauthier, J. et al. (2018) Recessive mutations in >VPS13D cause childhood onset movement disorders. Annals of neurology 83 (6), 1089-1095.

99. Darvish, H. et al. (2018) Identification of a large homozygous VPS13C deletion in a patient with early-onset Parkinsonism. Movement disorders : official journal of the Movement Disorder Society 33 (12), 1968-1970.
100. Lesage, S. et al. (2016) Loss of VPS13C Function in Autosomal-Recessive Parkinsonism Causes Mitochondrial Dysfunction and Increases PINK1/Parkin-Dependent Mitophagy. American journal of human genetics 98 (3), 500-513.
101. Kumar, N. et al. (2018) VPS13A and VPS13C are lipid transport proteins differentially localized at ER contact sites. The Journal of cell biology 217 (10), 3625-3639.
102. Marongiu, R. et al. (2009) Mutant Pink1 induces mitochondrial dysfunction in a neuronal cell model of Parkinson's disease by disturbing calcium flux. Journal of neurochemistry 108 (6), 1561-74.
103. Takenouchi, T. et al. (2001) Reduced neuritic outgrowth and cell adhesion in neuronal cells transfected with human alpha-synuclein. Molecular and cellular neurosciences 17 (1), 141-50.
104. Oliveira, L.M. et al. (2015) Elevated alpha-synuclein caused by SNCA gene triplication impairs neuronal differentiation and maturation in Parkinson's patient-derived induced pluripotent stem cells. Cell death & disease 6, e1994.
105. Lee, H.J. et al. (2012) alpha-Synuclein modulates neurite outgrowth by interacting with SPTBN1. Biochemical and biophysical research communications 424 (3), 497-502.
106. Kim, S. et al. (2018) Alpha-Synuclein Suppresses Retinoic Acid-Induced Neuronal Differentiation by Targeting the Glycogen Synthase Kinase-3beta/beta-Catenin Signaling Pathway. Molecular neurobiology 55 (2), 1607-1619.
107. Ronzitti, G. et al. (2014) Exogenous alpha-synuclein decreases raft partitioning of Cav2.2 channels inducing dopamine release. The Journal of neuroscience : the official journal of the Society for Neuroscience 34 (32), 10603-15.
108. Jensen, P.H. et al. (2000) Microtubule-associated protein 1B is a component of cortical Lewy bodies and binds alpha-synuclein filaments. The Journal of biological chemistry 275 (28), 21500-7.
109. Gai, W.P. et al. (1996) Microtubule-associated protein 5 is a component of Lewy bodies and Lewy neurites in the brainstem and forebrain regions affected in Parkinson's disease. Acta neuropathologica 91 (1), 78-81.
110. Baranov, S.V. et al. (2019) Mitochondria modulate programmed neuritic retraction. Proceedings of the National Academy of Sciences of the United States of America 116 (2), 650-659.
111. Dagda, R.K. et al. (2014) Beyond the mitochondrion: cytosolic PINK1 remodels dendrites through protein kinase A. Journal of neurochemistry 128 (6), 864-77.
112. Samann, J. et al. (2009) Caenorhabditits elegans LRK-1 and PINK-1 act antagonistically in stress response and neurite outgrowth. The Journal of biological chemistry 284 (24), 16482-91.
113. Azkona, G. et al. (2018) LRRK2 Expression Is Deregulated in Fibroblasts and Neurons from Parkinson Patients with Mutations in PINK1. Molecular neurobiology 55 (1), 506-516.
114. Lee, S. et al. (2010) LRRK2 kinase regulates synaptic morphology through distinct substrates at the presynaptic and postsynaptic compartments of the Drosophila neuromuscular junction. The Journal of neuroscience : the official journal of the Society for Neuroscience 30 (50), 16959-69.
115. Islam, M.S. et al. (2016) Human R1441C LRRK2 regulates the synaptic vesicle proteome and phosphoproteome in a Drosophila model of Parkinson's disease. Human molecular genetics 25 (24), 5365-5382.
116. Chan, S.L. et al. (2014) MAP1B rescues LRRK2 mutant-mediated cytotoxicity. Molecular brain 7, 29.
117. Safaei, R. and Fischer, I. (1989) Cloning of a cDNA encoding MAP1B in rat brain: regulation of mRNA levels during development. Journal of neurochemistry 52 (6), 1871-9.
118. Zhu, M. et al. (2015) Mask loss-of-function rescues mitochondrial impairment and muscle degeneration of Drosophila pink1 and parkin mutants. Human molecular genetics 24 (11), 3272-85.

119. Popelka, H. and Klionsky, D.J. (2018) Structural basis for extremely strong binding affinity of giant ankyrins to LC3/GABARAP and its application in the inhibition of autophagy. Autophagy 14 (11), 1847-1849.
120. Li, J. et al. (2018) Potent and specific Atg8-targeting autophagy inhibitory peptides from giant ankyrins. Nature chemical biology 14 (8), 778-787.
121. Klionsky, D.J. et al. (2016) Guidelines for the use and interpretation of assays for monitoring autophagy (3rd edition). Autophagy 12 (1), 1-222.
122. Wang, Q.J. et al. (2006) Induction of autophagy in axonal dystrophy and degeneration. The Journal of neuroscience : the official journal of the Society for Neuroscience 26 (31), 8057-68.

Figure and Table Legends:

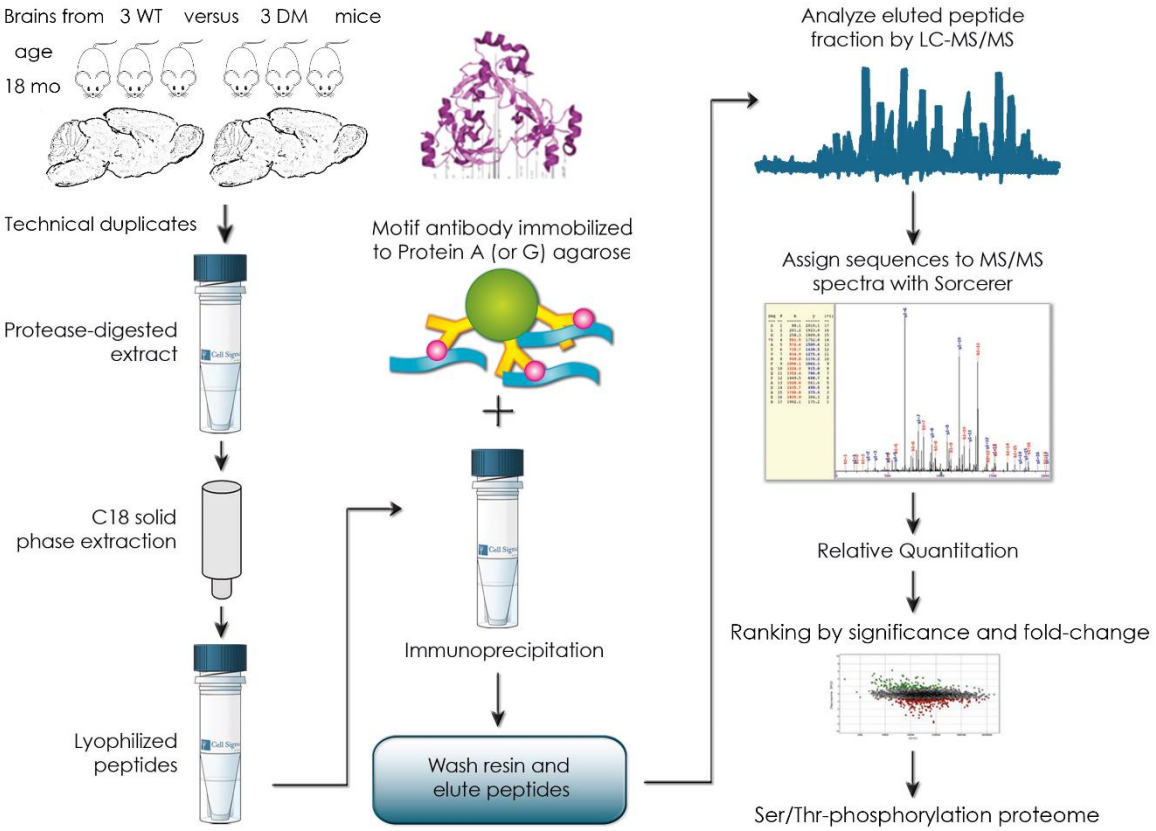

Figure 1: Flow chart illustrating the experimental approach to quantify the Ser/Thr-phosphorylation of trypsination-derived peptides from the global proteome of mouse brain. C18 solid phase extraction, lyophilization, immunoprecipitation with motif antibody (3D structure illustrated) immobilized on protein A (or G) agarose (beads shown as green circle, immunoglobulin coating in yellow, binding of digested peptides in blue with their Ser/Thr-phosphorylations in pink) and mass spectrometry in a quantitative and label-free manner were employed. Graphic elements from internet sites were used with permission of Cell Signaling Inc., see http://www.cellsignal.com/common/content/content.jsp?id=proteomics-discovery.

Preprints (www.preprints.org) | NOT PEER-REVIEWED | Posted: 7 June 2019 doi:10.20944/preprints201906.0052.v1

Peer-reviewed version available at *Int. J. Mol. Sci.* **2019**, *20*, 3284; doi:10.3390/ijms20133284

A

Normalized Fold Change					Max % CV					
DM all : Control	DM 1 : Control	DM 2 : Control	DM 3 : Control	Max Intensity	Biological	Gene Name	Protein Name	Site	Peptide	Count in Details
-314,3	-255,3	-438,7	-279,5	6.559.198	35,4	Mtap1b	MAP1B	§1928	TIKT*PEDGGYTCEITEK	16
-3,3	-543,3	-715,4	-1,1	858.179	155,1	Ank2	ANK2 iso2 + iso3	§3781; §3809; §872	GSPIVQEPEEASEPKEESS*PRK	29
-3,0	-1,0	-47,8	-31,0	947.741	143,6	Vps13d	VPS13D	§2429	NAS*SESAVVPK	8
-2,3	-2,9	-2,9	-1,6	26.223	54,5	Mtap2	MAP2 iso6	§1801; §471	RLSNVSSS*GSINLLESPQLATLAEDVTAALAK	3
-2,3	-2,9	-2,9	-1,6	26.223	54,5	Mtap2	MAP2 iso6	§1803; §473	RLSNVSSSGS*INLLESPQLATLAEDVTAALAK	3
-2,1	-2,1	-3,1	-1,4	436.205	32,6	Epb4.1l2	EPB41L2 iso3	§86	QRS*YNLVVAK	3
-1,9	-4,5	-1,5	-1,4	543.218	47,1	Dapk2	DAPK2	§299	RES*VVNLENFKK	11
-1,8	-2,2	-1,4	-2,0	27.656	33,9	Mark1	MARK1	§394, §403	SRPSS*DLNNSTLQS*PAHLK	19
-1,7	-2,1	-1,7	-1,4	405.747	33,8	Vps13c	VPS13C	2481	QESS*LFTLTFVPYGYTEVASVPVAR	5
-1,6	-1,2	-5,2	-1,1	400.265	53,3	Mtap1a	MAP1A	§1794	VPSAPGQESPVPDT*KSTPPTR	2
-1,6	-1,2	-5,2	-1,1	400.265	53,3	Mtap1a	MAP1A	1796	VPSAPGQESPVPDTKS*TPPTR	2
-1,6	-1,2	-5,2	-1,1	400.265	53,3	Mtap1a	MAP1A	§1797	VPSAPGQESPVPDTKST*PPTR	31
-1,6	-2,1	-1,4	-1,4	2.098.225	24,4	Kif1a; Kif1a	KIF1A iso3	§1537; §1540	SRPAS*PEPELLPELDSK	22
-1,4	-1,1	-2,6	-1,1	454.218	35,3	Mtap1a	MAP1A	§1789, 1796	VPSAPGQES*PVPDTKS*TPPTR	3
-1,4	-1,1	-2,6	-1,1	454.218	35,3	Mtap1a	MAP1A	§1789, §1797	VPSAPGQES*PVPDTKST*PPTR	43
1,5	2,0	1,5	1,1	674.946	30,3	Mapre2	RP1	§218, §222	SSPASKPGSTPS*RPSS*AK	11
1,6	2,3	1,5	1,1	563.552	32,4	Mapre2	RP1	§215, §222	SSPASKPGS*TPSRPSS*AK	2
1,7	1,8	2,1	1,3	12.258.948	25,6	Add2	ADD2	§528, §532, §535	S*RS*PS*TES*QLMSK	26
1,7	2,2	1,9	1,2	519.692	28,2	Mark1	MARK1	§504	RNT*YVCER	8
1,7	2,0	1,9	1,2	39.365	30,1	Clasp1	CLASP1 iso3	§646, §649	RQS*SGS*TTNVASTPSDSR	5
2,2	1,2	4,4	1,0	1.375.910	82,0	Epb4.1l1	EPB41L1 iso2 + iso4	§546; §545	RLPSSPASPS*PK	29

B

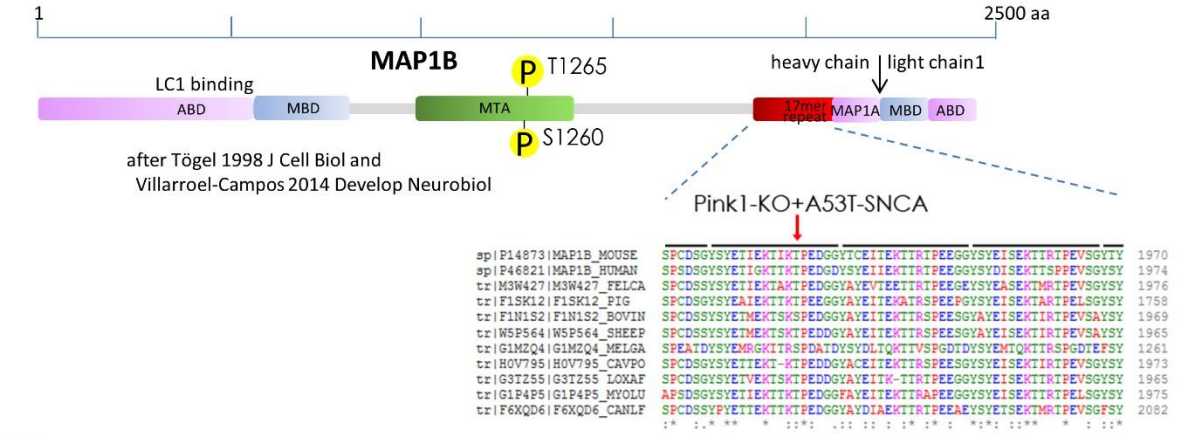

C

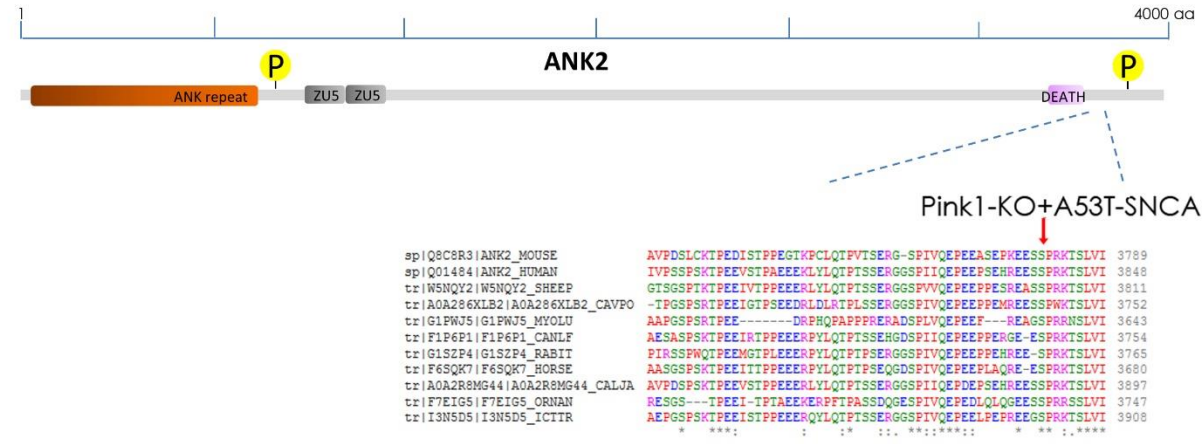

Figure 2: Phosphoproteomics reveals a cluster of dysregulations in factors associated with microtubules and microfilaments. **(A)** Selected list of phosphopeptides that showed a two-fold dysregulation at least once among the 3 biological replicates. The list presents also signal intensity and coefficient of variance (CV), the phosphorylation site, the peptide sequence with the phosphorylated residue (illustrated by asterisk *), and the peptide count. A selective

massive deficit of pT1928 in MAP1B and the second strongest deficit of pS3781 in ANK2 as a MAP1B-interactor were documented. These prominent changes clustered with an enrichment of factors that link the cytoskeleton to either the mitochondria or to the plasma membrane signaling apparatus, namely MAP2, EPB41L2 (4.1G), MARK1, MAP1A, KIF1A, RP1, ADD2, CLASP1 and EPB41L1 (4.1N). **(B)** Scheme of MAP1B protein sequence, cleavage into heavy chain and light chain 1 (LC1), structural motifs with their interactions [LC1 binding in heavy chain, actin binding domain ABD, microtubule binding domain MBD, microtubule assembly helping site MTA, region that contains 12 repeats of a 17mer sequence, MAP1A interacting domain] and characterized GSK3beta-dependent phospho-sites at pS1260 / pT1265, which have an established effect on cytoskeletal reorganization. Alignment of MAP1B protein sequences from mouse, man, cat (FELCA), pig, cattle (BOVIN), sheep, wild turkey (MELGA), guinea pig (CAVPO), African elephant (LOXAF), little brown bat (MYOLU) and dog (CANLF) illustrates the conservation of the *Pink1*-KO+A53T-SNCA-modulated Thr/Ser site (red arrow) within the 17mer repeat (highlighted as black bars above sequence) of unknown function. **(C)** Scheme of ANK2 protein sequence, structural motifs (Ankyrin repeat, ZU5 domains and DEATH domain, with characterized phosphorylation sites at S846 and S3850. Alignment of ANK2 protein sequences from mouse, man, sheep, guinea pig (CAVPO), little brown bat (MYOLU), dog (CANLF), rabbit, horse, marmoset (CALJA), duckbill platypus (ORNAN) and squirrel (ICTTR) illustrates the conservation of the *Pink1*-KO+A53T-SNCA-modulated Ser site (red arrow) within the C-terminal target interaction domain. For a complete list of the residues with potential phosphorylation, see www.phosphosite.org.

Preprints (www.preprints.org) | NOT PEER-REVIEWED | Posted: 7 June 2019 doi:10.20944/preprints201906.0052.v1

Peer-reviewed version available at *Int. J. Mol. Sci.* **2019**, *20*, 3284; doi:10.3390/ijms20133284

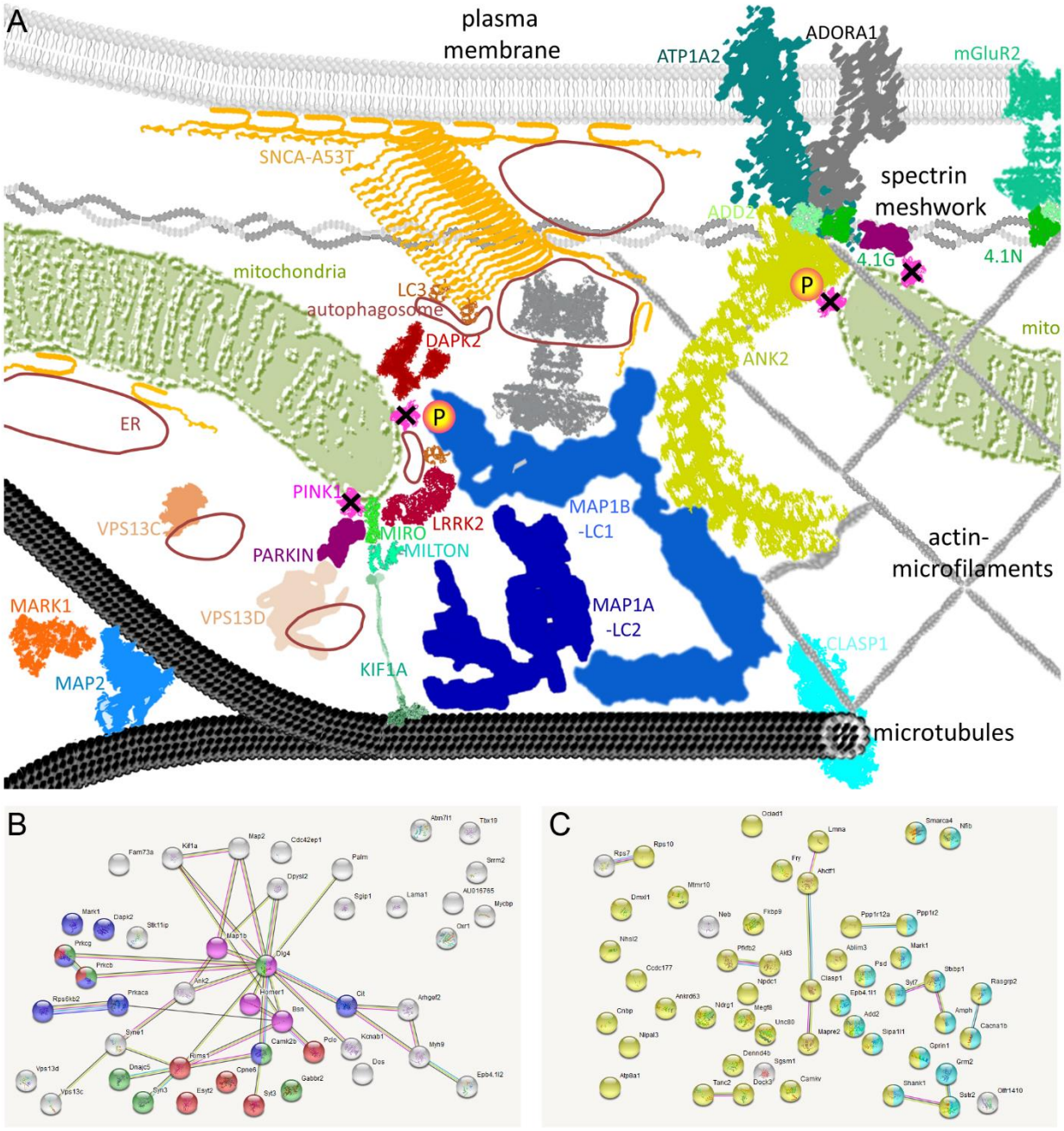

Figure 3: (A) Schematic representation of dysregulated factors, based on their subcellular localization and on textmining about functional interaction effects. Three cytoskeletal layers underlying neuronal plasma membranes (microtubules, actin-microfilaments, spectrin meshwork) are shown, which provide correct localization to mitochondria, vesicles and the membrane channels / pumps. The overexpressed mutant A53T-SNCA with its aggregates, the deleted PINK1 kinase and the downstream proteins affected by altered phosphorylation – and LRRK2 as a DAPK2 homologous kinase that phosphorylates MAP1B in abnormal manner in the PARK8 variant of PD – are visualized as colored symbols, reminiscent of their known 3D

structures and with rough representation of their size differences. The two strongest deficits in phosphorylation are highlighted in pink/yellow circles. As additional automated scheme on protein-protein interactions and pathway enrichments, STRING diagrams are provided for all **(B)** 45 factors with reduced Ser/Thr-phosphorylation and **(C)** 49 factors with increased Ser/Thr-phosphorylation. Significant bioinformatics enrichments were prominent for "Protein kinase C conserved region 2 (CalB)" among SMART protein domains (false discovery rate FDR = 4.09e-07) and for the "C2 domain" among INTERPRO and PFAM protein domains (FDR=5.18e-07) (illustrated as red bullets), for the "Serine/threonine-protein kinase, active site" among INTERPRO domains (FDR=9.14e-07) (blue bullets), for the "Transmission across chemical synapses" (FDR=8.78e-06) (green bullets) with particularly "Glutamate binding, activation of AMPA receptors and synapses" (FDR=1.74e-05), and for the article "Bodaleo-FJ et al 2016 Sci Rep" on MAP1B-deficiency effects on synaptic components (purple bullets) among the downregulations. Significant enrichments were detected only for the expected terms "phosphoprotein" (FDR=9.17e-14) (yellow bullets) and "neuron part" (FDR=2.48e-05) (light blue bullets). The protein-protein enrichment p-value was very significant among the downregulations (p=7.54e-12), but barely significant among the downregulations (p=0.036). Previous knowledge of the interaction between these factors from experiments, co-expression, or text mining is illustrated by connecting lines of various colors.

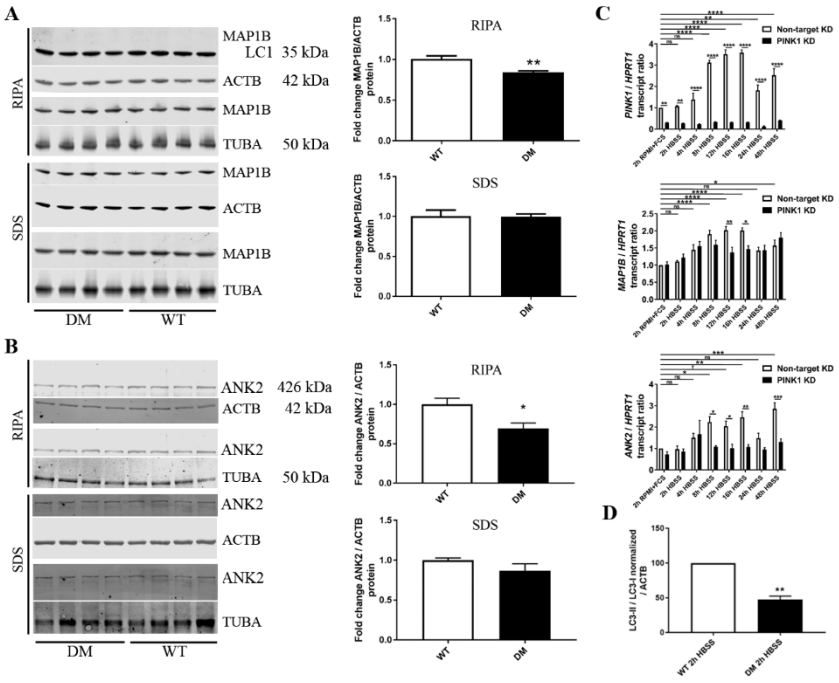

Figure 4: Validation experiments regarding expression modulation at protein and mRNA level. **(A)** Quantitative immunoblots detecting MAP1B relative to beta-actin (ATCB) as loading control and marker of the cortical actin cytoskeleton, or to alpha-tubulin (TUBA) as loading control and marker of the microtubular cytoskeleton, both for RIPA-soluble and for SDS-soluble fractions of the brain proteome. **(B)** Quantitative immunoblots detecting ANK2 relative to beta-actin (ATCB) as loading control or to alpha-tubulin (TUBA) as loading control, both for RIPA-soluble and for

SDS-soluble fractions of the brain proteome. **(C)** Transcript abundance of *PINK1* (above) and *MAP1B* (below), normalized to the loading control *HPRT1*, in human SH-SY5Y neuroblastoma cells undergoing nutrient deprivation in HBSS medium without fetal calf serum over a time course of 48 hours. Black bars represent cells with stable knock-down (KD) of *PINK1*, while white bars represent non-target (NT) knock-down controls. Starvation induces *PINK1* mRNA in phasic manner with a peak between 12 h and 16 h. MAP1B mRNA is induced in a similar pattern, but the induction is not maintained after 12 h in PINK1-KD cells (n= 4 *PINK1*-KD versus 4 NT-KD) **(D)** Quantitative immunoblots in primary cortical neurons (28 days *in vitro*) starved for 2 hours with HBSS medium show a significant reduction of the LC3-II isoform versus LC3-I in DM mice (n= 4 DM vs 4 WT, two litters).

Supplementary Table S1: Global mouse brain proteome phosphorylation with >2-fold dysregulation at least once among the biological triplicates, illustrating downregulations in red and upregulations in green, and emphasizing proteins with consistent >2-fold changes by a more intense coloring. Relevant bioinformatics and annotations for each phosphorylation site are provided in separate datasheets.

Supplementary Table S2: STRING Heidelberg database pathway enrichments among the proteins **(A)** of all downregulated and **(B)** of all upregulated phospho-sites.